

# Novel Design Theory for High-Efficiency and High-Linearity Microwave Power Amplifier Based on 2nd Harmonic: Enhanced Class-J

Seyed A. Mohadeskasaei, Fuhong Lin\*, Xianwei Zhou, and Sani U. Abdullah

**Abstract**—In this paper, after a brief review of the previous nonlinear power amplifier (PA) classes including Class-B, Class-F, and Class-J, a novel design theory for high-efficiency and high-linearity microwave power amplifier based on 2nd harmonic component of the drain voltage and current signals is proposed. The new scheme introduces a new nonlinear class which like Class-J tunes only two primary harmonic components but unlike Class-J, the drain voltage is boosted to the maximum four times dc drain voltage. A quasi half sinusoidal waveform for the current and a quadratic sinusoidal waveform for the voltage are thus realized in this class, leading to a minimum waveform overlapping. The new class theoretically provides 93% power efficiency. It is, in fact, an enhanced Class-J with higher power efficiency and better linearity performance.

## 1. INTRODUCTION

A power amplifier is one of the most important components of a communication system. Modern signal modulations such as LTE and LTE-A have stimulated the rapid progress of PA designs. PA features, such as bandwidth, power efficiency, and linearity performance, are finely considered in modern modulations more than traditional modulations, thus causing a detail research and development in the PA design. PA performances are limited by either its design theory or the active device's technologies. Fortunately, the device's technologies have been well developed recently, allowing the proposition of new PA structures based on tuning higher harmonic components.

So far, many PAs topologies including linear and nonlinear classes have been introduced. In the linear classes (Class-A, Class-B, and Class-AB) [1–3], load network (matching network) is usually as a low-pass filter, creating a full sinusoidal waveform for the drain voltage and a dedicated waveform for the drain current in the face of a full sinusoidal at Class-A or a half-sinusoidal at Class-B or a quasi-half sinusoidal at Class-AB. As a result, higher harmonic components of the voltage signal are not generated due to a shorted-circuit condition provided by the low-pass filter (load network) at harmonic frequencies. Hence, linear class of PAs show meritorious linearity performance, unlike their low efficiency which is due to the permanent overlap between the drain voltage and current signals. Although the theory of synthesis of a load network by a low-pass filter for linear class of PAs seems simple, in fact, an ideal shorted-circuit condition for all higher harmonics is hard to realize, thus tending to the presence of undesired higher harmonic components of the voltage and current signals and degrading efficiency and linearity performance.

The nonlinear classes including Class-D, Class-E [4, 5], Class-F/F-1 [6, 7], and Class-J [8–10] are recommended for high efficiency applications. In these classes, load network creates minimum possible overlap between the voltage and current waveforms, which eliminates power dissipation and enhances

---

*Received 31 March 2017, Accepted 26 May 2017, Scheduled 8 June 2017*

\* Corresponding author: Fuhong Lin (B20130548@xs.ustb.edu.cn).

The authors are with the School of Computer and Communication Engineering, University of Science and Technology Beijing, Beijing 100083, P. R. China.

power efficiency. To provide this condition, at least three early harmonic components of voltage for Class-F/F-1 and Class-E, and two early harmonic components for Class-J are compulsory tuned. Class-F/F-1 and Class-E are in fact able to theoretically provide 100% drain efficiency by using an infinite number of higher harmonic components while particularly sacrificing linearity performance. Class-J with better linearity performance than Class-F/F-1 and even Class-E provides maximum power efficiency as high as 78.5% theoretically.

Recently, Class-J PA is taken into account more because of its acceptable compromise between power efficiency and linearity performance while unlike Class-B scheme, second harmonic is not entirely removed, and thus, it provides a feasibility to design of high-efficiency broadband PA [9]. The advantage of Class-J in comparison with Class-B in narrow bandwidth applications is slight [8]. In this concept, the drain voltage and current waveforms contain only two first harmonic components, eliminating shorted-circuit condition at the second harmonic. The maximum drain voltage may be three times of dc drain voltage, limiting designers to use any kind of transistor [11]. Fortunately, among today's technologies, GaN HEMT with high breakdown voltage and high band gap can be considered for this class operation [12]. The load impedance must be purely capacitive in Class-J PA, while even if a zero-loss load network is employed, the device output resistance ( $R_{DS}$ ) reported in HEMTs is still present and cannot practically be lifted.

In this paper, we propose a novel class scheme for microwave PA which is an enhanced Class-J. In this class, both aforementioned restrictions on a shorted-circuit condition (like Class-B scheme) and/or a purely capacitive load at a second harmonic (like Class-J scheme) are lifted. Two primary higher harmonics of the drain voltage and current signals are tuned so that quasi-half-sinusoidal waveforms with minimum feasible overlap for the drain voltage and current appear. The maximum drain voltage can nearly reach four times of dc drain voltage, providing an useful advantage which can obtain higher output power from the lower dc supply voltage. The maximum drain efficiency will be 93% in the proposed operation class theoretically. Thus, this class in comparison with Class-J provides higher efficiency and unlike Class-F/F-1 and Class-E tuned until third harmonic, takes only two early harmonic components, enabling it to be especially useful for ultra-frequency high-efficiency applications.

The rest of the paper is organized as follows. In Section 2, previous nonlinear classes including Class-B, Class-F, and Class-J are briefly reviewed. In Section 3, the design theory of a new class (enhanced Class-J) is proposed and compared with the previous class scheme in detail. Lastly, the paper is concluded and compared with other PA classes in Section 4.

## 2. NON-LINEAR CLASS CONCEPTS

In this section, the previous concepts of high-efficiency nonlinear classes including Class-B, Class-F, and Class-J are briefly reviewed. Since Class-E shows highly nonlinear behavior due to acting transistor as a switch, it is not a worthwhile scheme for PA working in microwave frequency ranges especially in applications relying on simultaneous high-efficiency and high linearity performance.

High-efficiency operation is fulfilled by two basic concepts. First, the power dissipation at the fundamental and harmonic frequencies is minimized. Second, the output power at the fundamental frequency is maximized. The first one is realized when the overlap between the drain voltage and current waveforms is reduced. For this reason, the PA is biased at the pinch-off point to provide a half-sinusoidal waveform for a half cycle of the current signal with zero value for another half cycle. From a Fourier's series expansion point of view, the drain current is expressed as

$$i_{d,B}(\omega t) = I_{\max} \left( \frac{1}{\pi} - \frac{1}{2} \sin(\omega t) - \frac{2}{\pi} \sum_{n=2,4,6,\dots}^{\infty} \frac{\cos(n\omega t)}{n^2 - 1} \right) \quad (1)$$

where  $I_{\max}$  denotes the maximum drain current, and  $n$  stands for the number of harmonic components. An infinite number of harmonics must be employed to make an ideal half-sinusoidal waveform.

### 2.1. Class-B Scheme

A half-sinusoidal waveform shown in Eq. (1) for the drain current and a full sinusoidal waveform for the drain voltage are realized for a Class-B PA by a proper load network. The normalized drain voltage is

therefore represented as

$$v_{d,B}(\omega t) = (V_{dd} - V_k)(1 + \sin(\omega t)) \tag{2}$$

where  $V_{dd}$  and  $V_k$  are denoted for the drain dc bias voltage and device knee voltage, respectively. Using Eqs. (1) and (2) for the drain current and voltage signals, the output powers at the dc, fundamental, and higher harmonics become

$$P_{dc,B} = \frac{(V_{dd} - V_k) I_{\max}}{\pi} \tag{3}$$

$$P_{out,B}|_{@f_0} = \frac{(V_{dd} - V_k) I_{\max}}{4} \tag{4}$$

$$P_{out,B}|_{@nf_0} = 0 \text{ for } n > 1 \tag{5}$$

The drain efficiency for PA working in Class-B scheme is estimated to be  $\eta_B = \pi/4\% \cong 78.5\%$ . To achieve such efficiency, PA must be derived so that the output power attains nearly 1-dB gain comparison point, showing that this scheme is far from a high-linearity operation (Class-A). The normalized drain voltage and current waveforms as well as an ideal Class-B PA load line are shown in Figs. 1 and 2. The load network impedance at the fundamental and harmonic frequencies to estimate Eqs. (1) and (2) must be as

$$Z_{L,B@f_0} = \frac{2(V_{dd} - V_k)}{I_{\max}} \tag{6}$$

$$Z_{L,B@nf_0} = 0 \text{ for } n > 1 \tag{7}$$

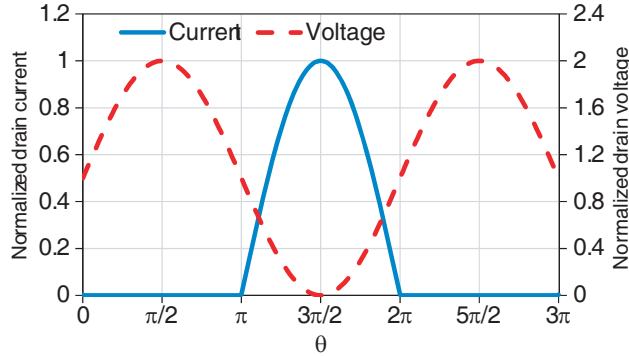


**Figure 1.** Normalized voltage and current waveforms for Class-B PA.

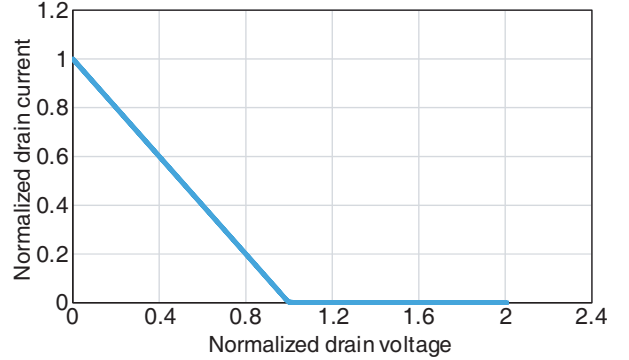


**Figure 2.** Generic load line of Class-B PA.

Therefore, to fulfill half-sinusoidal for current and full-sinusoidal for voltage waveforms, output network must provide a purely resistive load at the fundamental ( $Z_{L,B@f_0} = R_{L,B@f_0}$ ) and zero impedance (short circuit) at all higher harmonics for the device. However, the device parasitic elements (output capacitance and resistance) do not practically allow the estimation of such conditions, especially at the early harmonic frequencies.

### 2.2. Class-F Scheme

The Class-F scheme has been firstly introduced by Cripps [13] and Raab [14]. In Class-F, as what has already been mentioned in Class-B, PA is biased at the pinch-off point, enabling it to make a half-sinusoidal waveform represented in Eq. (1) for the current signal. The load network must theoretically consist of an infinite number of resonator circuits to trap all even harmonic components. The drain voltage is thus assumed as

$$v_{d,F}(\omega t) = (V_{dd} - V_k) \left( 1 + \frac{4}{\pi} \sin(\omega t) + \frac{4}{3\pi} \sin(3\omega t) + \frac{4}{5\pi} \sin(5\omega t) + \dots \right) \tag{8}$$

where  $V_{dd}$  and  $V_k$ , similar to the definitions of Class-B, are denoted for the drain dc bias voltage and device knee voltage, respectively. The output powers at the dc, fundamental, and third harmonic components while supposing Eqs. (1) and (8) for the drain current and voltage waveforms become

$$P_{dc,F} = \frac{(V_{dd} - V_k) I_{\max}}{\pi} = P_{dc,B} \quad (9)$$

$$P_{out,F}|_{@f_0} = \frac{(V_{dd} - V_k) I_{\max}}{\pi} = \frac{2}{\pi} P_{out,B}|_{@f_0} \quad (10)$$

$$P_{out,F}|_{@nf_0} = 0 \text{ for } n > 1, \quad (11)$$

showing the possibility of drain efficiency of 100% ( $P_{dc,F} = P_{out,F@f_0}$ ). The output power at the fundamental frequency is slightly less than Class-B, requiring that the bias point is increased forward to the deep Class-AB. In comparison with Class-B, this scheme is also taken farther from the high-linearity operation, since, in practice, such a large second harmonic component coefficient ( $4/3\pi$ ) in comparison with the fundamental ( $4/\pi$ ) is provided as PA is derived with a large input signal and taken forward to more than 1-dB compression point. From a practical point of view, using an infinite number of resonator circuits to engineer Eq. (8) is unfeasible, and therefore, a limited number of harmonics, e.g., until third or fifth ones, are tuned. The normalized waveforms and load lines with different harmonic components of Class-F PA in comparison with Class-B are shown in Figs. 3 and 4. The load network estimating Eqs. (1) and (8) must see impedances at the fundamental and harmonic frequencies as,

$$Z_{L,F@f_0} = \frac{8(V_{dd} - V_k)}{\pi I_{\max}} = \frac{4}{\pi} R_{L,B@f_0} \quad (12)$$

$$Z_{L,F@nf_0} = 0 \text{ For } n = 2, 4, 6, \dots \quad (13)$$

$$Z_{L,F@nf_0} = \infty \text{ For } n = 3, 5, 7, \dots \quad (14)$$

As can be understood from Eqs. (12)–(14), the load network must be realized as a purely resistive load at the fundamental frequency, while looking a shorted-circuit condition at the even harmonic frequencies and an opened-circuit condition at the odd ones. In microwave frequencies, a conquering capacitive load ( $C_{DS}$ ) impedance is small enough to prevent practically synthesizing opened-circuit conditions. On the other hand, as already mentioned while explaining Class-B issue, even if the load network is designed as a short circuit at all even harmonics,  $C_{DS}$  and  $R_{DS}$  are still present, introducing another limitation for implementing the Class-F load network. At the microwave frequencies, Class-F PA is in fact tuned by only three early harmonics, theoretically tending to maximum drain efficiency of 88% (10% improvement rather than Class-B) [15]. However, to estimate terminations which provide a necessary non-overlap condition for the drain and voltage waveforms, power at the harmonic frequencies is generated, certainly degrading the maximum efficiency to under 82% [16].

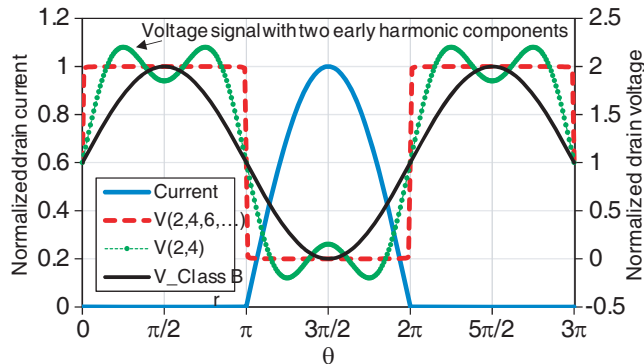


**Figure 3.** Normalized voltage and current waveforms for a generic Class-F PA with an infinite number of harmonics and only two early harmonics in comparison with Class-B PA waveforms.

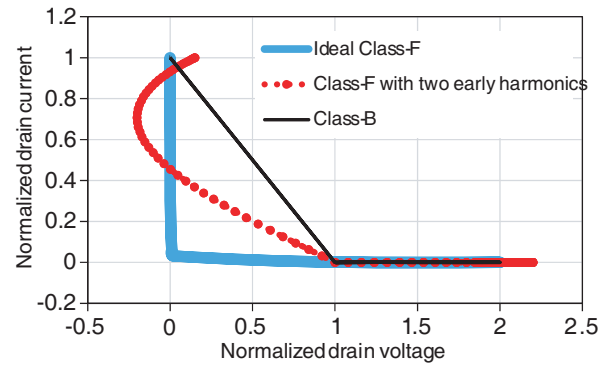


**Figure 4.** Ideal load lines of a class-F PA with an infinite number of harmonics and only two early harmonics in comparison with Class-B PA load line.

### 2.3. Class-J Scheme

Class-J PA scheme [6] originates from Class-B PA while taking only two primary harmonic components of the drain current shown in Eq. (1). A proper load network is employed to shift voltage described for Class-B as long as the phase difference is between  $45^\circ$ . The drain voltage and current waveforms as the result become

$$i_{d,J}(\omega t) = I_{\max} \left( \frac{1}{\pi} - \frac{1}{2} \sin(\omega t) - \frac{2}{3\pi} \cos(2\omega t) \right) \quad (15)$$

$$v_{d,J}(\omega t) = \underbrace{(V_{dd} - V_k)(1 + \sin(\omega t))}_{\text{Class-B voltage signal}} \underbrace{(1 + \alpha \cos(\omega t))}_{\substack{\text{corresponding term} \\ \text{to shift the voltage} \\ \text{waveform}}} \quad (16)$$

where  $\alpha$  is defined as the constant coefficient limited in  $[-1, 1]$ .

With some manipulations and using  $\sin(\alpha) \cos(\alpha) = 0.5 \sin(2\alpha)$ , the drain voltage presented in Eq. (16) can be rewritten as

$$v_{d,J}(\theta) = (V_{dd} - V_k)(1 + \sin(\omega t) + \alpha \cos(\omega t) + 0.5\alpha \sin(2\omega t)) \quad (17)$$

The active output powers at the dc, fundamental, and higher harmonic components are thus obtained as

$$P_{dc,J} = \frac{(V_{dd} - V_k) I_{\max}}{\pi} = P_{dc,B} \quad (18)$$

$$P_{out,J}|_{@f_0} = \frac{(V_{dd} - V_k) I_{\max}}{4} = P_{out,B}|_{@f_0} \quad (19)$$

$$P_{out,J}|_{@2f_0} = 0 \quad (20)$$

Therefore, the drain efficiency becomes as high as  $\eta_J = 78.5\%$ . The output power and efficiency are therefore similar to that of Class-B. The reactive power generated at the second harmonic indicates as heat and dissipation.

Fortunately, in this class, unlike Class-F, the need to feed PA by a large level signal for generating large second harmonic coefficient has been lifted. Typically, the nonlinear behavior of  $C_{DS}$  aims to generate second harmonic component, and it is hence possible to expect better linearity performance than Class-F and even Class-B at the lower input power level (closer to Class-A). The corresponding load impedances at the fundamental and second harmonic in such a way that Eqs. (1) and (15) are realized are as follows;

$$Z_{L,J@f_0} = \frac{2(V_{dd} - V_k)}{I_{\max}}(1 + j\alpha) = R_{L,B@f_0} + j\alpha R_{L,B@f_0} \quad (21)$$

$$Z_{L,J@2f_0} = -j \frac{3\pi}{8} \frac{2\alpha(V_{dd} - V_k)}{I_{\max}} = -j \frac{3\pi}{8} R_{L,B@f_0} \quad (22)$$

As can be inferred from Eq. (22), the load impedance at the second harmonic must be a purely capacitive load, removing the need for shorted- or opened-circuit conditions as already relying on it in the later cases. As a result, this scheme potentially offers a wide-band operation structure suited for high-efficiency broadband applications. However in practice, even if the output matching network loss is ignored, the device output resistance ( $R_{DS}$ ) prevent from providing a purely capacitive load. The voltage and current waveforms for the groups of Class-J (the different values of  $\alpha$ ) in comparison with Class-B are shown in Fig. 5. The ideal load lines of Class-J PA for different values of  $\alpha$  are shown in Fig. 6.

### 2.4. Enhanced Class-J Scheme

A Class-J scheme is enhanced so that, like Class-J, only two early harmonic components of Eq. (1) are taken, but unlike Class-J, the drain voltage is not only shifted but also pulled up to four times higher than drain dc supply as a result of a proper load network. It requires to select value under a quarter

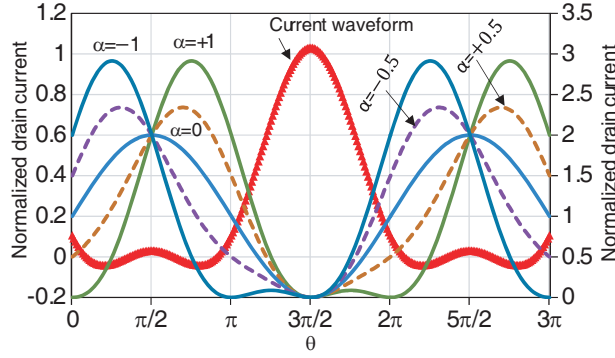


**Figure 5.** Normalized voltage and current waveforms for a generic Class-J PA for different values of  $\alpha$ .

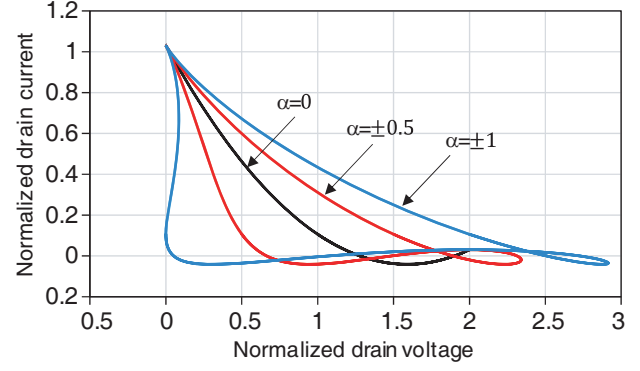


**Figure 6.** Ideal load lines of Class-J PA for different values of  $\alpha$ .

of breakdown voltage for drain dc bias point for the transistor. The current and voltage waveforms in this class are defined as:

$$i_{d,EJ}(\omega t) = I_{\max} \left( \frac{1}{\pi} - \frac{1}{2} \sin(\omega t) - \frac{2}{3\pi} \cos(2\omega t) \right) \quad (23)$$

$$v_{d,EJ}(\omega t) = \underbrace{(V_{dd} - V_k)(1 + \sin(\omega t))}_{\text{Class-B voltage signal}} \underbrace{(1 + \alpha \cos(\omega t + \varphi))}_{\text{corresponding term to shift and rise the voltage waveform}} \quad (24)$$

where  $\alpha$  and  $\varphi$  are the constant parameters with different signs bounded in the two ranges of  $\{-1, 0\}$  &  $[0, \pi/2\}$  and  $\{[0, 1] \text{ \& } [-\pi/2, 0]\}$ , respectively. Equation (24) for  $\alpha = 0$  demonstrates Class-B waveform and for  $\varphi = 0$  makes Class-J waveforms. Using  $\cos(\alpha + \beta) = \cos(\alpha)\cos(\beta) - \sin(\alpha)\sin(\beta)$ ,  $\sin(\alpha)\cos(\alpha) = 0.5\sin(2\alpha)$ , and  $\sin^2(\alpha) = 0.5(1 - \cos(2\alpha))$ , and with some manipulations, the drain voltage presented in Eq. (24) can be rewritten as

$$v_{d,EJ}(\omega t) = (V_{dd} - V_k) \left[ \underbrace{1 - \frac{\alpha}{2} \sin(\varphi)}_{\text{dc term}} + \underbrace{\alpha \cos(\varphi) \cos(\omega t) + (1 - \alpha \sin(\varphi)) \sin(\omega t)}_{\text{Fundamental harmonic component}} + \underbrace{\frac{\alpha \cos(\varphi)}{2} \sin(2\omega t) + \frac{\alpha \sin(\varphi)}{2} \cos(2\omega t)}_{\text{Second harmonic component}} \right] \quad (25)$$

The normalized voltage and current waveforms of enhanced Class-J PA for different values of  $\alpha$  and  $\varphi$  are depicted in Fig. 7. The note which must be taken into account is that the maximum drain voltage can reach four times of dc drain voltage, and thus to avoid breakdown, less than a quarter of breakdown voltage of active device can be a proper bias point for this class PA. The active output powers at the dc, fundamental, and higher harmonic components are thus obtained from Eqs. (23)–(25) as;

$$P_{dc,EJ} = \frac{(V_{dd} - V_k) I_{\max}}{\pi} (1 + 0.5\alpha \sin(\varphi)) = P_{dc,B} (1 + 0.5\alpha \sin(\varphi)) \quad (26)$$

$$P_{out,EJ}|_{@f_0} = \frac{(V_{dd} - V_k) I_{\max}}{4} (1 - \alpha \sin(\varphi)) = (1 - \alpha \sin(\varphi)) P_{out,B}|_{@f_0} \quad (27)$$

$$P_{out,EJ}|_{@2f_0} = \frac{(V_{dd} - V_k)(\alpha \sin(\varphi))}{6\pi I_{\max}} \quad (28)$$

The output power, as can be understood from Eq. (26), can receive two times higher than output power of Class-B for  $\{\alpha = +1 \text{ \& } \varphi = -\pi/2\}$  and/or  $\{\alpha = -1 \text{ \& } \varphi = \pi/2\}$ . It also demonstrates

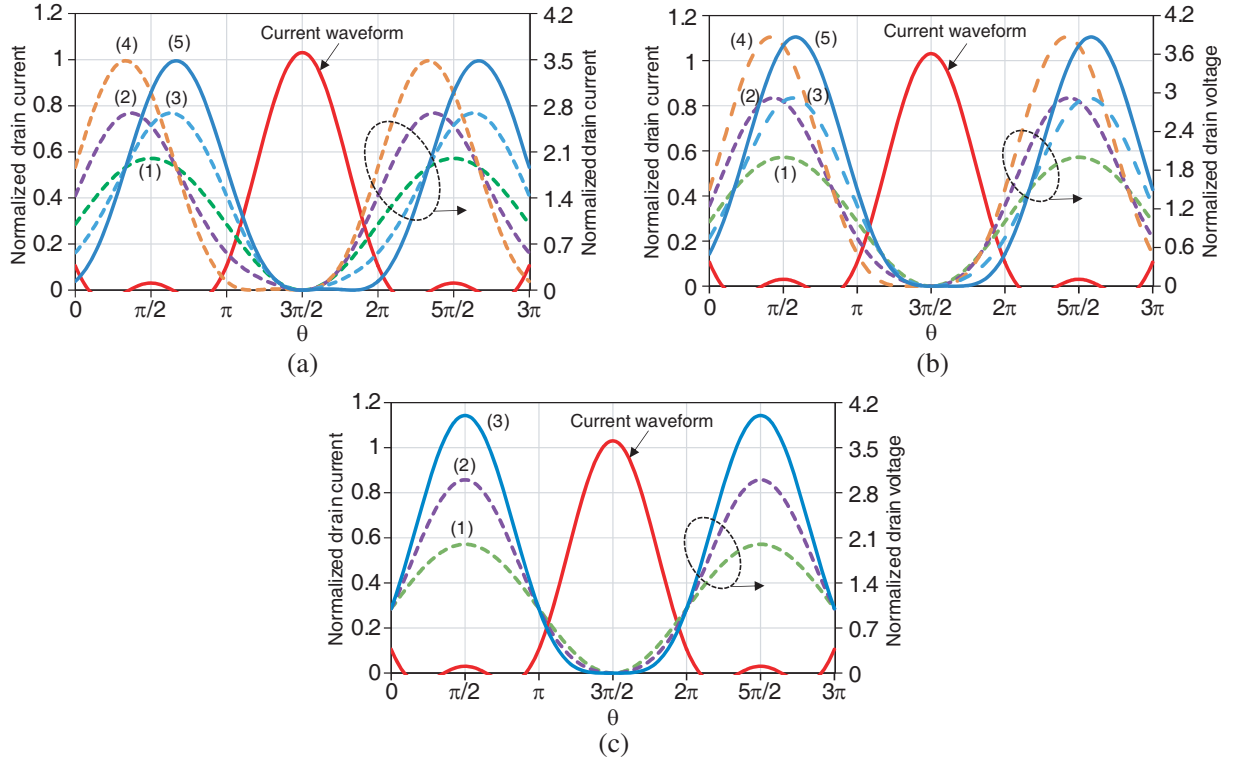


**Figure 7.** Normalized voltage and current waveforms for different values of  $\alpha$  and  $\varphi$ . (a) (1)  $\alpha = 0$  &  $\varphi = \mp\pi/6$ , (2)  $\alpha = 0.5$  &  $\varphi = -\pi/6$ , (3)  $\alpha = -0.5$  &  $\varphi = \pi/6$ , (4)  $\alpha = 1$  &  $\varphi = -\pi/6$ , (5)  $\alpha = -1$  &  $\varphi = \pi/6$ . (b) (1)  $\alpha = 0$  &  $\varphi = \mp\pi/3$ , (2)  $\alpha = 0.5$  &  $\varphi = -\pi/3$ , (3)  $\alpha = -0.5$  &  $\varphi = \pi/3$ , (4)  $\alpha = 1$  &  $\varphi = -\pi/3$ , (5)  $\alpha = -1$  &  $\varphi = \pi/3$ . (c) (1)  $\alpha = \pm 1$  &  $\varphi = \mp\pi/2$ , (2)  $\alpha = \pm 0.5$  &  $\varphi = \mp\pi/2$ , (3)  $\alpha = 0$  &  $\varphi = \mp\pi/2$ .

that this class scheme in comparison with the other already presented classes provides much better linearity performance (closer to Class-A rather than all), since higher signal gain before clipping signal will be provided in the new class. A 3-D view of normalized fundamental output power by dividing the  $P_{out,B@f_0}$  as functions of  $\alpha$  and  $\varphi$  is depicted in Fig. 8. The ideal load lines as functions of  $\alpha$  and  $\varphi$  are depicted in Fig. 9.

The average drain efficiency is thus simply calculated from Eqs. (26)–(28) as

$$\eta = 100 \frac{\pi}{4} \left( \frac{1 - \left(1 - \frac{2}{3\pi}\right) \alpha \sin(\phi)}{1 - 0.5\alpha \sin(\varphi)} \right) \% \quad (29)$$

The 2-D and 3-D views of drain efficiency as the functions of  $\alpha$  and  $\varphi$  are depicted in Fig. 10. The drain efficiency attains 93% at  $\{\alpha = 1 \text{ \& } \varphi = -\pi/2\}$  and  $\{\alpha = -1 \text{ \& } \varphi = \pi/2\}$ , showing better efficiency than Class-B, Class-J, and even Class-F with three trapped-harmonic components. The load impedance at the fundamental and second harmonic satisfying Eqs. (23) and (24) must be

$$Z_{L,EJ@f_0} = \frac{2(V_{dd} - V_k)}{I_{\max}} (1 - \alpha \sin(\varphi) - j\alpha \cos(\varphi)) \quad (30)$$

$$Z_{L,EJ@2f_0} = \frac{3\pi}{2} \frac{(V_{dd} - V_k)}{I_{\max}} \left( \frac{\alpha}{2} \sin(\varphi) - j\frac{\alpha}{2} \cos(\varphi) \right) \quad (31)$$

As we mentioned while explaining Class-B and Class-J schemes,  $C_{DS}$  and  $R_{DS}$  are permanently presence, and therefore, load impedance as a complex load at fundamental and second harmonic is more feasible than a real impedance (Class-B) or a purely capacitive impedance (Class-J).



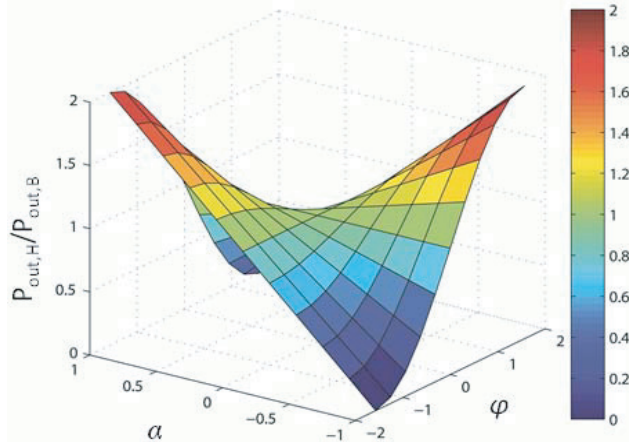


**Figure 8.** 3-D view of normalized output power of enhanced Class-J PA as functions of  $\alpha$  and  $\varphi$ .

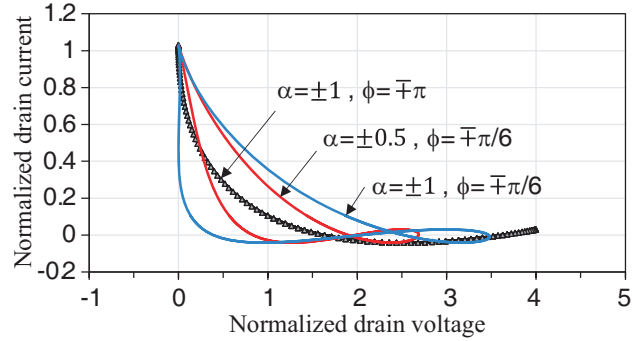


**Figure 9.** Ideal load-line of enhanced Class-J for different values of  $\alpha$  and  $\varphi$ .

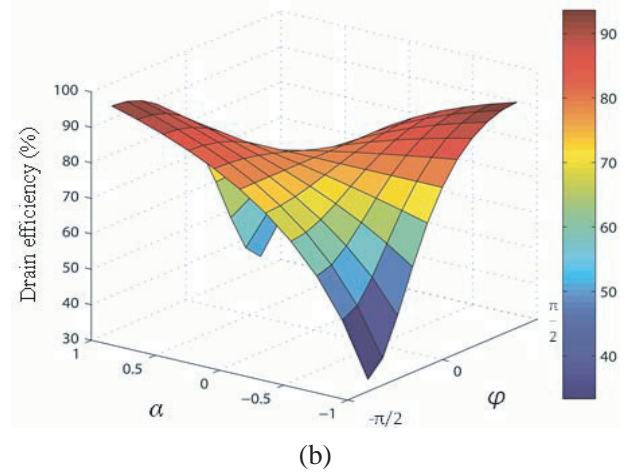
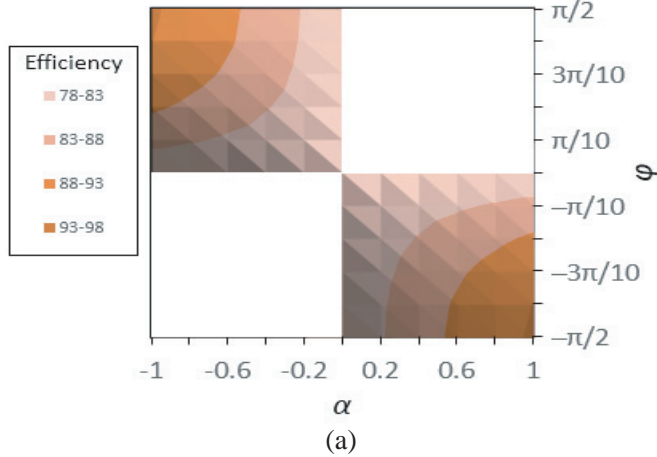


**Figure 10.** Drain efficiency for enhanced Class-J as the functions of  $\alpha$  and  $\varphi$ , (a) contour graph, (b) 3-D view.

### 3. CONCLUSION

In this paper, the previous nonlinear PA classes including Class-B, Class-F, and Class-J are briefly reviewed, and then, a novel nonlinear PA class (enhanced Class-J) is proposed and shows that the main limitations in the other state of the high-efficiency PA structures including opened-circuit and shorted-circuit conditions for Class-B and Class-F/F-1, or a purely capacitive load at the second harmonic frequency for Class-J are lifted. It is theoretically expected that PA designed in this operating class provides output power as high as two times of Class-B output power and attains 93% of power efficiency.

### ACKNOWLEDGMENT

This work is supported by the National Natural Science Foundation of P. R. China (U1603116).



## REFERENCES

1. Cripps, S. C., P. J. Tasker, A. L. Clarke, J. Lees, and J. Benedikt, "On the continuity of high efficiency modes in linear RF power amplifiers," *IEEE Microwave and Wireless Components Letters*, Vol. 19, No. 10, 665–667, Oct. 2009.
2. Seyed Alireza Mohadeskasaei, S. U. A., J. An, Y. Chen, Z. Li, and T. Sun, "Systematic approach for design of broadband, high efficiency, high power RF amplifiers," *ETRI Journal*, Vol. 39, No. 1, 51–61, Feb. 2017.
3. Zhao, D. and P. Reynaert, "A 60-GHz dual-mode class AB power amplifier in 40-nm CMOS," *IEEE Journal of Solid-State Circuits*, Vol. 48, No. 10, 2323–2337, Oct. 2013.
4. Chen, K. and D. Peroulis, "Design of highly efficient broadband Class-E power amplifier using synthesized low-pass matching networks," *IEEE Transactions on Microwave Theory and Techniques*, Vol. 59, No. 12, 3162–3173, Dec. 2011.
5. Grebennikov, A., "High-efficiency class-E power amplifier with shunt capacitance and shunt filter," *IEEE Transactions on Circuits and Systems I: Regular Papers*, Vol. 63, No. 1, 12–22, Jan. 2016.
6. Kim, J. H., G. D. Jo, J. H. Oh, Y. H. Kim, K. C. Lee, and J. H. Jung, "Modeling and design methodology of high-efficiency Class-F and Class-F-1 power amplifiers," *IEEE Transactions on Microwave Theory and Techniques*, Vol. 59, No. 1, 153–165, Jan. 2011.
7. Hayati, M., A. Sheikhi, and A. Grebennikov, "Class-F power amplifier with high power added efficiency using bowtie-shaped harmonic control circuit," *IEEE Microwave and Wireless Components Letters*, Vol. 25, No. 2, 133–135, Feb. 2015.
8. Moon, J., J. Kim, and B. Kim, "Investigation of a Class-J power amplifier with a nonlinear  $C_{out}$  for optimized operation," *IEEE Transactions on Microwave Theory and Techniques*, Vol. 58, No. 11, 2800–2811, Nov. 2010.
9. Wright, P., J. Lees, J. Benedikt, P. J. Tasker, and S. C. Cripps, "A methodology for realizing high efficiency Class-J in a linear and broadband PA," *IEEE Transactions on Microwave Theory and Techniques*, Vol. 57, No. 12, 3196–3204, Dec. 2009.
10. Park, S., J. L. Woo, U. Kim, and Y. Kwon, "Broadband CMOS stacked RF power amplifier using reconfigurable interstage network for wideband envelope tracking," *IEEE Transactions on Microwave Theory and Techniques*, Vol. 63, No. 4, 1174–1185, Apr. 2015.
11. Mohadeskasaei, S. A., F. Lin, X. Zhou, S. U. Abdullahi, and A. Ahmat, "Design of broadband, high-efficiency, and high-linearity GaN HEMT Class-J RF power amplifier," *Progress In Electromagnetics Research C*, Vol. 72, 177–186, 2017.
12. Jin, H., Q. Li, L. Zhang, X. Zeng, and R. Yang, "Review of wide band-gap semiconductors technology," *MATEC Web of Conferences*, Vol. 40, 2016.
13. Cripps, S. C., *RF Power Amplifiers for Wireless Communications*, Artech House, 1999.
14. Raab, F. H., "Class-F power amplifiers with maximally flat waveforms," *IEEE Transactions on Microwave Theory and Techniques*, Vol. 45, No. 11, 2007–2012, 1997.
15. Rudiakova, A. and V. Krizhanovski, *Advanced Design Techniques for RF Power Amplifiers*, Springer, 2006.
16. Colantonio, P., F. Giannini, and E. Limiti, *High Efficiency RF and Microwave Solid State Power Amplifiers*, John Wiley and Sons, 2009.